Journal of Power Sources 556 (2023) 232429

Contents lists available at ScienceDirect

Journal of Power Sources

journal homepage: www.elsevier.com/locate/jpowsour

A novel semi-supervised learning approach for State of Health monitoring of maritime lithium-ion batteries

Clara Bertinelli Salucci [a,*], Azzeddine Bakdi [a,b], Ingrid Kristine Glad [a], Erik Vanem [a,c], Riccardo De Bin [a]

[a] University of Oslo, Department of Mathematics, Moltke Moes vei 35, Oslo, 0851, Norway
[b] Corvus Energy, Tormod Gjestlands veg 51, Porsgrunn, 3936, Norway
[c] DNV Group Technology and Research, Veritasveien 1, Høvik, 1322, Norway

HIGHLIGHTS

- A novel semi-supervised method for on/offline battery health monitoring is presented.
- The approach is developed with real usage data from the maritime field.
- The method is versatile and provides sensible results, in line with expectations.
- A cumulative model is applied on labels generated with this approach with low errors.

ARTICLE INFO

Keywords:
State of Health monitoring
Maritime battery systems
Data-driven modelling
Semi-supervised learning
Multivariable Fractional Polynomial regression

ABSTRACT

Lithium-ion batteries are a prominent technology for the electrification of the transport sector, which itself is a key measure towards the departure from fossil fuels. The "green shift" is taking place in the marine industry too, where the number of battery-powered vessels is fastly growing. In this case, monitoring the battery State of Health is essential more than ever to optimise battery use, promote safety, and ensure the coverage of ship power and energy demands. Classification societies typically require annual capacity tests for this purpose; however, the tests are disruptive, costly and time-consuming. As a consequence they are seldom, in addition to not being always fully reliable. We propose a novel alternative semi-supervised learning approach to estimate the State of Health of a lithium-ion battery system with no labelled data, starting from a minimal set of weakly labelled data from another similar system. The method is based on operational sensor data gathered from the battery, together with the battery State of Charge. Our results show that the procedure is valid, and the obtained estimates can be used to significantly progress in failure prevention, operational optimisation, and for planning batteries at the design stage.

1. Introduction

It is commonly recognised that the electrification of the transportation sector is a key measure towards the departure from fossil fuels. The need for a so-called "green shift" concerns the shipping sector importantly: it has been estimated that CO_2 emissions from international shipping are 2.5% of the global total, and the impact of ships emission can get up to be 55%–77% of the total in port regions [1]. Battery-powered (fully electric or hybrid) ships represent an attractive alternative which is already in place in many shipping segments (e.g. ferries, offshore supply vessels). Lithium-ion (Li-ion) batteries are currently the predominant technology, due to the important advantages they have compared to other battery types [2]. In particular, concerning maritime applications, batteries reduce shipping emissions and costs due to improved energy efficiency and reduced maintenance requirements. However, it is crucial to have a reliable method to estimate and monitor the battery conditions, especially because Li-ion batteries age over years and usage, resulting in both energy and power fade [3]. Monitoring of the battery State of Health (SoH) is essential for the battery system protection, e.g. detecting the battery End of Life (EoL), determining the available battery power and energy capacity for reliable ship operation. The SoH is usually defined on the basis of either the battery resistance, maximum power, or discharge capacity: in this study we consider the capacity-based

* Corresponding author.
E-mail addresses: clarabe@math.uio.no (C. Bertinelli Salucci), azzeddib@math.uio.no (A. Bakdi), glad@math.uio.no (I.K. Glad), erik.vanem@dnv.com (E. Vanem), debin@math.uio.no (R. De Bin).

https://doi.org/10.1016/j.jpowsour.2022.232429
Received 18 July 2022; Received in revised form 27 October 2022; Accepted 15 November 2022
Available online 29 November 2022

definition, which is the most commonly adopted, and hence denote the SoH as

$$\mathrm{SoH}_i = \frac{C_{\mathrm{available}}}{C_{\mathrm{nominal}}} \times 100\,(\%), \tag{1}$$

where $C_{\mathrm{available}}$ is the remaining capacity, and C_{nominal} is the nominal capacity of the battery system. Both capacities are typically measured using standard charge and discharge methods. Note that the actual initial capacity is often used in the place of the nominal capacity, especially when the analysis is not conducted on the system as a whole, but at the cell (smallest unit) level.

Estimating the remaining battery capacity is not an easy task in itself. Ship classification societies usually require periodic (often annual) independent tests to verify the battery conditions. Such tests enable capacity estimation, but are disruptive, time consuming, and difficult to perform under controlled conditions similar to lab conditions. Hence, the often sparse independent tests provide only a general indication of the battery real SoH. These considerations motivate the research of alternative approaches to monitor the SoH of maritime battery systems.

A promising direction is provided by data-driven models, based on operational sensor data from the battery systems. As opposed to model-based methods, which consider the physics of deterioration to model the battery degradation with e.g. equivalent circuits, data-driven methods sidestep the involved physical processes (which are complex, interacting, and not fully modelled in the literature) by approximating physical relations with a great advantage in flexibility and, often, computability. Further remarks on the categorisation in model-based or data-driven approaches, which is not the only possible one and is often interpreted in different ways, can be found in the reviews by Basia et al. [4], Yao et al. [5], Tian et al. [6], Barre et al. [7]. Cuma and Koroglu [8] classify into model-based and other various methodologies such as genetic algorithms, fuzzy logic, neural networks, extended Kalman filters and dynamic Bayesian networks. Electrochemical model-based methods are discussed by Farmann et al. [9], together with voltage-based estimation methods, incremental capacity analysis/differential voltage analysis methods and ageing prediction methods. A different categorisation, distinguishing between experimental techniques and adaptive battery models, can be found in the critical review by Berecibar et al. [10], while Li et al. [11] discriminate data-driven models as being characterised by: either model-fitted features, depending on an underlying state space model; or processed external features, e.g. extracted from differential voltage curves; or direct external features, directly measured by sensors, such as voltage, current and temperature.

A complete overview of the data-driven techniques for SoH modelling, with particular focus on maritime applications, is provided by Vanem et al. [3]. The authors categorise data-driven methods into: direct measurements techniques, state-space models with observers, regression type models, time-series models, survival type models, cumulative damage models, and empirical or analytical models. A characteristic that is common to many of the listed approaches is the need of time-series of SoH measurements, which are typically not available in practice. Therefore, methods that provide capacity estimations only based on the continuous sensor data are described as hugely advantageous. The availability of big volumes of data together with the sparsity of independent SoH tests motivate the novel approach we present in this paper, which has the aim of combining the information from a few labelled data-points with the considerable amount of unlabelled sensor data gathered during the ships operation.

Despite the abundant research on SoH estimation of Li-ion batteries, which is not yet considered to be exhaustive (see e.g. [11]), most of the literature has focused on fully supervised models that are trained using sufficient labelled data samples, relying mainly on accelerated ageing tests. Very few papers have considered the different and common problems of missing or limited labelled samples in filed data. Xiong et al. [12] proposed capacity prediction using Electrochemical Impedance Spectroscopy (EIS) data in case of missing capacity measurements; the proposed neural network was trained on a subset of capacity and EIS labelled samples. However, EIS data is not continuously available in practice, due to EIS testing impact on operation and lifetime. Considering limited labels, Che et al. [13] presented a semi-supervised self-learning-based methodology for lifetime prediction based on experimental data. Li et al. [14] proposed a transfer learning approach by finding dissimilarities in data samples through maximum mean discrepancy; this algorithm was trained on lab data including capacity characterisation cycles. Transfer learning on lab data was also employed by Deng et al. [15] and by Li et al. [16]: in the first case, degradation patterns are classified using an unsupervised methodology and transfer learning is applied to a short long-term memory neural network; in the latter, transfer learning assists a pruned convolutional neural network. In a similar setup and using locally linear reconstruction, Yu et al. [17] proposed an oversampling method that creates labels for the unlabelled training samples based on similarities with limited labelled training data to train a SoH predictive model. Wu and Li [18] proposed a combination of encoder and decoder neural networks to learn then reconstruct features in partial cycles based on training data of full cycles; this method has also been trained on lab data with full characterisation cycles. Diao et al. [19] considered a different problem for binary classification of battery ageing patterns under missing labels of abnormal degradation; the proposed method (support vector machine) was trained using only normal ageing labelled data to detect anomalous degradation.

To the best of our knowledge, the algorithm presented in this paper is the first algorithm developed for SoH estimation of nearly unlabelled data from real usage of battery systems. The remainder of this article is organised as follows: Section 2 provides a brief description of the characteristics typical of maritime battery systems and of the datasets at hand; Section 3 describes our semi-supervised learning method; in Section 4 we present and discuss the results obtained with operational data from different vessels; Section 5 discusses the methodology and provides concluding remarks.

2. Data description

2.1. Maritime battery systems

Large-format battery systems such as the maritime batteries are characterised by several differences, compared to the setup of simple battery-powered items such as flashlights or consumer electronics. However, since the degradation mechanisms of a specific cell-type are the same if cycled under the same conditions, it is likely for a method to be easily adaptable to a number of different battery application fields. Yet, when it comes to generalisation of a method developed on maritime batteries, it is important to consider that the specific battery design and usage profile do have an impact on the methods and models adopted: for example, the design influences the battery management system, protection limits, and thermal management, while the usage profile determines charge/discharge C-rates, depth of discharge (DoD), temperature, rest periods. It seems therefore relevant to outline the main characteristics of the large battery systems designed for maritime applications that are the object of this study. The two main differences between small and large battery systems are identified by Weicker [20] as: the much higher number of battery cells (the smallest electrochemical unit); and the more complex interactions between the battery itself and the load device. Further, a generic maritime battery system can be described at different levels [21]:

- cell: smallest energy storage unit;
- module: ensemble of serial connected cells or cell blocks (parallel connected cells), often equipped by electronic monitoring and/or protective devices;

- string/pack: series of modules having the same voltage as the system (overall) level, can serve as a standalone energy storage unit or be connected in parallel with other packs;
- battery system: unit composed of one or several battery packs and equipped with all the necessary monitoring, control and protective systems. These are typically integrated in the Battery Management System (BMS), which ensures safe conditions and operations.

Additionally, maritime battery systems are equipped with many layers of protection from cell to battery system, such as ventilation, cooling and fire protection apparatus, as their typical high voltages and high currents make them linked to much larger hazards than the smaller systems.

The availability of data from the battery system at different levels (cell, module, pack) poses the dilemma about which level should the SoH estimation be made at, both with respect to computability and accuracy, as well as generalisability. The answer is non-trivial, since the level choice depends on the type of data available, but also because the level preference is likely to influence the modelling phase. For the present case we have decided to carry the analysis at the pack level, as it seemed the most convenient choice given the data at our disposal; however, it is well known that battery systems are inescapably characterised by cell-to-cell variations and imbalance [22] and by temperature differences: all this might result in significant differences in the SoH across one system subunit.

2.2. Dataset description

The operational data at hand are provided by Corvus Energy and consist of high-frequency sensor data from three vessels (vessels A, B, and C) powered by battery systems with similar cell type and module design, but different sizes and usage profiles. They comprise time-series of current, temperature, voltage and State of Charge (SoC)—we take the liberty of treating the SoC as sensor data insofar as it was provided by the data supplier with good accuracy. All variables are continuously over the time span of the available datasets, 4.5 to 5.5 years, though periods of missing data are present in each of the three cases. Rough estimates for the amount of days without data are: 43% for vessel A, 15% for vessel B, and 9% for vessel C. Very few tests have been carried out to estimate the capacity, and hence the SoH, of the battery systems: the lack of a reasonable amount of SoH observations, together with the availability of a considerable volume of sensor data, motivates a semi-supervised learning approach that aims at maximising the information we can extract from the data. In this case, we work with a minimal set of weakly labelled data obtained by three SoH tests carried out on one of the vessels in three different years, two of which are non consecutive. The sensor data have been pre-processed to identify discharge phases on the basis of changes of sign in the SoC derivative: this enabled to go from continuous measurements in the four dimensions – current, temperature, voltage, SoC – to sequences of single events, namely the discharge cycles. Fig. 1 displays SoC data for a few days of operations: the charge and discharge phases are correctly identified by the pre-processing algorithm, which is designed to ignore small fluctuations due to noise in the data. The gap in the figure is due to missing data, a common characteristic of real data gathered during ship operation, which is to some extent accounted for in the analysis and briefly discussed. Summary statistics of the sensor data gathered during a discharge cycle encode its characteristics. These include: average C-rate, temperature range, Depth of Discharge (DoD), SoC range, total duration; other relevant properties are specified in Section 3.1.1. The method is comprised of two main parts: label learning and cumulative modelling. All cycles with DoD $= \Delta\text{SoC} \leq 10\%$ or duration shorter than five minutes were considered too shallow for the labelling phase, and hence neglected. We refer to Section 3.1.1 for other filtering criteria.

Data pertaining to vessel A, the ship provided with the three SoH tests and with the largest rate of missing data, will be referred to as *reference data*: the labelled discharge cycles from this vessel constitute the references we build the analysis on. Since there are only three SoH tests for the reference data, only three reference discharge cycles are labelled. However, we will assume the SoH to be constant in a time window around each test (Section 3), so that all the reference cycles in the window achieve a label too, i.e. the SoH value observed at the test (Fig. 2). The other two vessels, B and C, are our *target data*: we aim at estimating the battery SoH in correspondence with as many target cycles as possible. We refer to Table 1 for a clarification and reminder of the terminology used throughout the article. The resulting SoH estimates can be used as labels to convert target data into train and test data for further modelling, e.g. for cumulative degradation models, as we do in this paper, or for anomalous degradation detection as in [19].

Table 1
Brief glossary for the adopted terminology.

Cycle characteristics	A set of features describing a cycle, extracted from the sensor data gathered during the cycle.
Reference cycles	*Any* discharge from the reference dataset (vessel A, with three SoH tests), provided that it took place in a time-window around one of the tests. Reference cycles within each time-window share the same label, but potentially different characteristics.
Target cycles	Discharge cycles from the target datasets (vessels B & C) where we want to estimate the SoH.
Nominal cycles	Cycles that are performed at standard conditions (e.g. lab tests), hence suitable for capacity estimation. Such cycles are not identically observed in real-operation scenarios, hence the need for alternative SoH estimation methods.
Cycle group	Ensemble of reference and target cycles sharing the same characteristics: DoD, average C-rate, temperature range, etc. All cycles in the group are occurrences, at different time points, of reference or target cycles with the same characteristics. Two different groups will differ in at least one of the cycle characteristics.

Fig. 3 provides a visual representation of the data and the various phases of our methodology, which is explained in the next section of the article. In another setup, reference data can be replaced by lab cycling data, and target data cover all operating battery-driven vessels for a given battery design.

3. Methodology

Machine learning algorithms are methods that, given a set of input variables $\boldsymbol{x} = x_1, \ldots, x_p$ and an output variable y, allow to construct a learner, or rule, $f(\boldsymbol{x})$ that represents the best mapping of the input variables to the output. The rule will then enable predictions $\hat{y}$ of the response for new values of the input variables. In our case, the output variable Y (or response) is the SoH obtained from the actual capacity of a battery system from maritime applications, as from Eq. (1). The input variables are the *characteristics* of the discharge cycles, based on the sensor data that were gathered during each cycle. However, since the vast majority of the cycles lack a corresponding SoH observation, we cannot train a machine learning model to learn the rule $f(\boldsymbol{x})$ and enable SoH prediction. To overcome the issue, we developed the semi-supervised learning method which is described in this section.

The first phase of the method is label learning and it is based on detecting, matching, analysing, and modelling the characteristics of incomplete cycles around the reference SoH tests. It is based on the assumption that the SoH of the battery system can be considered constant for a time window of N days around the independent SoH test. This assertion is valid where considerable degradation takes several years, as in the case of this study: in practical applications, especially in the maritime field, the sudden drop in SoH (knee point) is often not reached and the battery decay is gentle and slow [23]. Nevertheless,

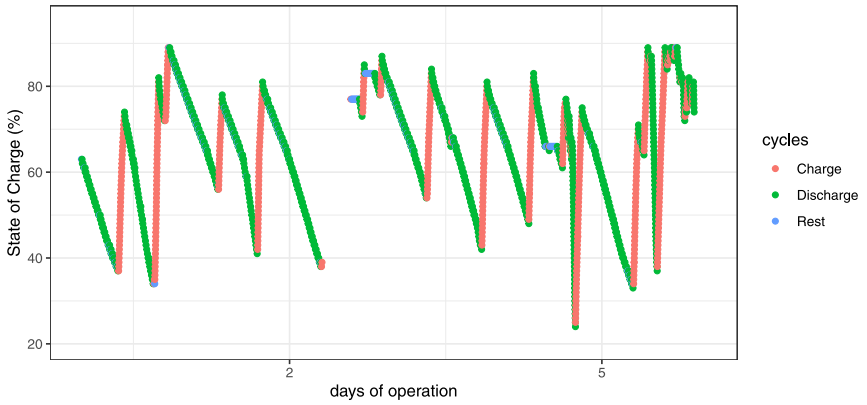

Fig. 1. State of Charge for one pack of vessel A, for a few days of operations: charge and discharge cycles have been identified in phase of pre-processing, and small fluctuations within a cycle have been ignored. The gap in the time-series is due to missing data in real operation scenarios. (For interpretation of the references to colour in this figure legend, the reader is referred to the web version of this article.)

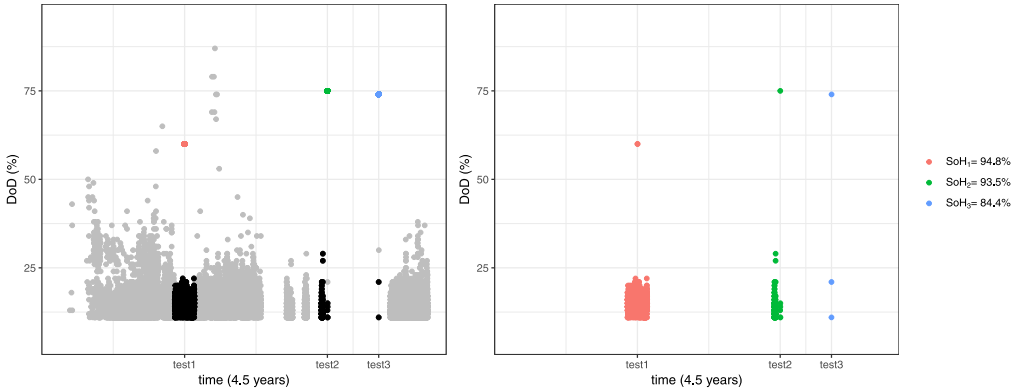

Fig. 2. Reference discharge cycles for one battery pack, DoD vs. initial timestamp. Left panel: the black dots are cycles taking place in the constant-SoH windows around the SoH tests, grey dots are cycles not included in such windows; only three cycles are labelled (coloured dots), as a consequence of having only three SoH tests. Right panel: the assumption of constant SoH enables us to enlarge the pool of labelled data points, since all cycles in the window are labelled with the SoH estimated at the SoH test; all cycles outside the windows are discarded. (For interpretation of the references to colour in this figure legend, the reader is referred to the web version of this article.)

the value of N should be chosen and adjusted depending on the specific data at hand. This fundamental assumption enables to enlarge the set of cycles with an associated label, to the advantage of the procedure.

The main limitation characterising real operation scenarios is that we never observe *nominal cycles*, i.e. cycles that are performed at standard conditions defined by the manufacturer: they require standard charge and discharge methods under specific C-rate, cutoff voltage and current, and temperature condition. If we could find nominal cycles in the operational history of the battery systems, we would be able to estimate the capacity directly by means of the Coulomb counting method [3,24]

$$C_{\text{available}} = \int_{t_0}^{t_1} \eta\, I(\tau)\, d\tau, \tag{2}$$

where t_0 and t_1 are the initial and final times of the complete discharge of the battery systems, $I(t)$ is the current intensity which evolves over time, and η is the Coulombic efficiency which is often assumed to be $\eta = 1$, as we do throughout the rest of this paper.

The conditions of the nominal cycles are obviously not met in practice, and we do not observe any complete discharge, both because it would pose problems of operation limits (i.e. mission profile) and because discharging the battery system completely would contribute to accelerating the battery degradation itself. Then, the basic idea of our method is that, since we do have accurate State of Charge estimates at our disposal, we can use a slight modification of Eq. (2) as a *pseudo capacity* measurement, a yardstick to relate discharge cycles happening at relatively homogeneous conditions while the battery system ages over years. In formula,

$$C_{\text{pseudo}} = \int_{t_{\text{start}}}^{t_{\text{end}}} I(\tau)\, d\tau, \tag{3}$$

where t_{start} and t_{end} are now the start and end times of an incomplete, not nominal, discharge cycle from $\text{SoC}_{\text{start}}$ to SoC_{end}.

The two phases of the procedure, *label learning from incomplete cycles* and *cumulative modelling*, are described in the remainder of this section.

3.1. Label learning from incomplete cycles

The first phase of the semi-supervised learning approach in turn consists of two steps: *cycle clustering* and *SoH labelling*.

3.1.1. Cycle clustering

A crucial requisite for the method success is that the incomplete discharge cycles we relate take place under homogeneous conditions with respect to DoD, SoC range, C-rates and temperatures: in fact, different conditions have a large impact on capacity estimation, see e.g. [25]. The first step of the procedure is then identifying groups of cycles that happen at similar conditions, relatively constant, in the reference data. The adopted criteria for filtering and clustering the cycles are:

- Same DoD = $\text{SoC}_{\text{start}} - \text{SoC}_{\text{end}}$ ($\pm 2\%$ on each SoC measurement)
- Same $\text{SoC}_{\text{start}}$ ($\pm 2\%$)
- Same average C-rate (± 0.05)

- Variance over time in the C-rate below 0.15
- Same maximum and minimum temperature ±2.5 °C
- Variance over time in the temperature below 1 $(°C)^2$
- Variance over space (within the pack) in the temperature below 3.5 $(°C)^2$

The three last points, which are related to the temperature, are better specified in the reminder of this subsection. Note that conducting the analysis at the pack level and considering only cycles that are frequently repeated has important implications when it comes to the temperatures: variations in the temperatures from module to module, and across different cells inside a module. Therefore, in the case of a battery pack with n modules and k temperature sensors within each module, our way to aggregate the temperature data is as follows. We first compute summary statistics of temperature data for each module $i = 1, \dots, n$ and each sensor $j = 1, \dots, k$:

$$\begin{array}{ll} \mu_{t,ij} & \text{average over time for the single sensor} \\ \sigma^2_{t,ij} & \text{variance over time for the single sensor} \\ T_{\min,ij}, T_{\max,ij} & \text{min and max values for the single sensor.} \end{array} \tag{4}$$

The variance over time at the pack level is then obtained as

$$\bar{\sigma}^2_t = \frac{1}{k \cdot n} \sum_{l=1}^{k \cdot n} \sigma^2_{t,l}. \tag{5}$$

To account for differences across the modules, we first define the module average temperature by averaging over the k sensors in the module,

$$\bar{\mu}_{t,i} = \frac{1}{k} \sum_{j=1}^{k} \mu_{t,j} \qquad \text{for } i = 1, \dots, n. \tag{6}$$

The pack mean temperature is then the average of the module averages,

$$\tilde{\mu}^{\text{pack}}_t = \frac{1}{n} \sum_{i=1}^{n} \bar{\mu}_{t,i}. \tag{7}$$

Consequently, the variance over space (i.e. across modules) is obtained as

$$\hat{\sigma}^2_{\tilde{\mu}^{\text{pack}}_t} = \frac{1}{n-1} \sum_{i=1}^{n} (\bar{\mu}_{t,i} - \tilde{\mu}^{\text{pack}}_t)^2. \tag{8}$$

Finally, the minimum (maximum) values at the pack level are defined as the median values of the distribution of minimum (maximum) temperatures at the module level:

$$\begin{aligned} T^{\text{pack}}_{\min} &= \underset{i \in [1,n]}{\text{median}} \{T^{(i)}_{\min}\} \quad \text{with} \quad T^{(i)}_{\min} = \min_{j \in [1,k]} \{T^{(ij)}_{\min}\} \quad \text{for } i = 1, \dots, n \\ T^{\text{pack}}_{\max} &= \underset{i \in [1,n]}{\text{median}} \{T^{(i)}_{\max}\} \quad \text{with} \quad T^{(i)}_{\max} = \max_{j \in [1,k]} \{T^{(ij)}_{\max}\} \quad \text{for } i = 1, \dots, n. \end{aligned} \tag{9}$$

At the end of the cycle grouping, cycles with spurious data are further filtered out by requiring

$$0.6 \cdot C_{\text{nominal}} \leq \frac{\Delta t \cdot |\bar{I}|}{\text{DoD}} \leq 1.2 \cdot C_{\text{nominal}}, \tag{10}$$

where C_{nominal} is the nominal capacity of the battery system, Δt is the cycle duration, $|\bar{I}|$ is the cycle average current intensity (in absolute value), and $\text{DoD} = \text{SoC}_1 - \text{SoC}_2$ is the cycle Depth of Discharge.

This phase of the procedure leads to the identification of the *reference cycles*: cycles from the constant-SoH windows in the reference data (hence with an associated label), each with specific characteristics in terms of DoD, C-rates, temperatures and SoC range. Having found k groups of cycles means having identified k types of typical reference cycles with different characteristics: we underline the importance of analysing each group *per se* to adjust for the impact of different characteristics/conditions on capacity estimation. Within each group, each reference cycle will hopefully have several *occurrences* (the more, the better). *Target cycles* are cycles in the target data that have the same characteristics as the reference cycles. *Groups* of cycles are clusters of cycles, both in the reference and in the target data, sharing the same characteristics: each group can be thought as characterised by an archetype reference cycle and all cycles in that group are occurrences of either reference or target cycles with the same characteristics as the archetype. Groups containing only reference cycles are discarded, since the lack of targets makes such groups useless for the purpose of capacity estimation in the target datasets. Similarly, groups with less than five reference cycles are discarded, since such a small number of data points is insufficient for training a model for the SoH labelling and/or estimation; the other groups are treated independently from each other in the rest of the procedure.

3.1.2. SoH labelling

Suppose that q groups of cycles were identified (and not discarded) during the cycle classification phase: each group has a certain number $\mathcal{N} \geq 5$ of reference cycles, for which the capacity of the battery is assumed to be known, being the one estimated from the independent SoH tests. In this phase, q different linear models [26] are trained on the reference cycles, one for each class, to learn the relationship f between the observed capacity of the battery and a vector of input $\boldsymbol{x}$ that depends on the number of available reference cycles $\mathcal{N}$:

- for $\mathcal{N} < 7$: $\boldsymbol{x} = \{C_{\text{pseudo}}, t_{\text{start}}, \Delta t\}$,
  where C_{pseudo} is the pseudo-capacity defined in Eq. (3), t_{start} is the unix timestamp of the cycle start, and Δt is the cycle duration in seconds;
- for $\mathcal{N} = 7$: $\boldsymbol{x} = \{C_{\text{pseudo}}, t_{\text{start}}, \Delta t, \bar{\sigma}^2_t, \sigma^2_{\text{C-rate}}\}$,
  i.e. the temperature variance over time $\bar{\sigma}^2_t$ defined in Eq. (5) and the C-rate variance over time $\sigma^2_{\text{C-rate}}$ are added to the model;
- for $\mathcal{N} = 8$: $\boldsymbol{x} = \{C_{\text{pseudo}}, t_{\text{start}}, \Delta t, \bar{\sigma}^2_t, \sigma^2_{\text{C-rate}}, \bar{T}^{\text{pack}}\}$,
  i.e. the average pack temperature of the cycle $\bar{T}^{\text{pack}}$ also enters the model;
- for $\mathcal{N} > 8$: $\boldsymbol{x} = \{C_{\text{pseudo}}, t_{\text{start}}, \Delta t, \bar{\sigma}^2_t, \sigma^2_{\text{C-rate}}, T^{\text{pack}}_{\min}, T^{\text{pack}}_{\max}\}$,
  where the average pack temperature of the cycle $\bar{T}^{\text{pack}}$ is replaced by the maximum and minimum pack temperature values $T^{\text{pack}}_{\min}$ and $T^{\text{pack}}_{\max}$.

Thus, the capacity of the battery C (and, hence, the battery SoH) can be predicted from the input $\boldsymbol{x}$ using the learnt rule $\hat{f}$:

$$\begin{aligned} \hat{C} &= \hat{f}(C_{pseudo}, t_{\text{start}}, \Delta t, \dots) = \\ &= \hat{\beta}_0 + \hat{\beta}_1 C_{pseudo} + \hat{\beta}_2 t_{\text{start}} + \hat{\beta}_3 \Delta t + \cdots \end{aligned} \tag{11}$$

For each model, uncertainty on the capacity estimates can be further estimated [26] from the training (labelled) data:

$$\hat{s} = \sqrt{\frac{(C - \hat{C})^2}{n - p}} \tag{12}$$

where C is the observed capacity, n is the number of observations and p is the cardinality of $\boldsymbol{x}$.

Of the q resulting models, we want to keep only the ones having a reasonable amount of variability in the outcome explained by the model, and discard the others (implying that their corresponding groups of cycles are removed from the analysis). For this purpose, one option is to consider the *adjusted coefficient of determination* R^2_{adj} [27]: all models with R^2_{adj} below a given threshold are discarded. The threshold value can be adjusted manually in order to guarantee having enough data: in cases with many cycle groups and large amounts of matches in the target data, a high threshold can be selected to ensure accuracy; otherwise, some accuracy can be traded with larger amounts of estimates.

The capacity estimates from the different groups are then gathered together and converted to the SoH scale by dividing by the nominal capacity of the battery system. Since in real applications it is often

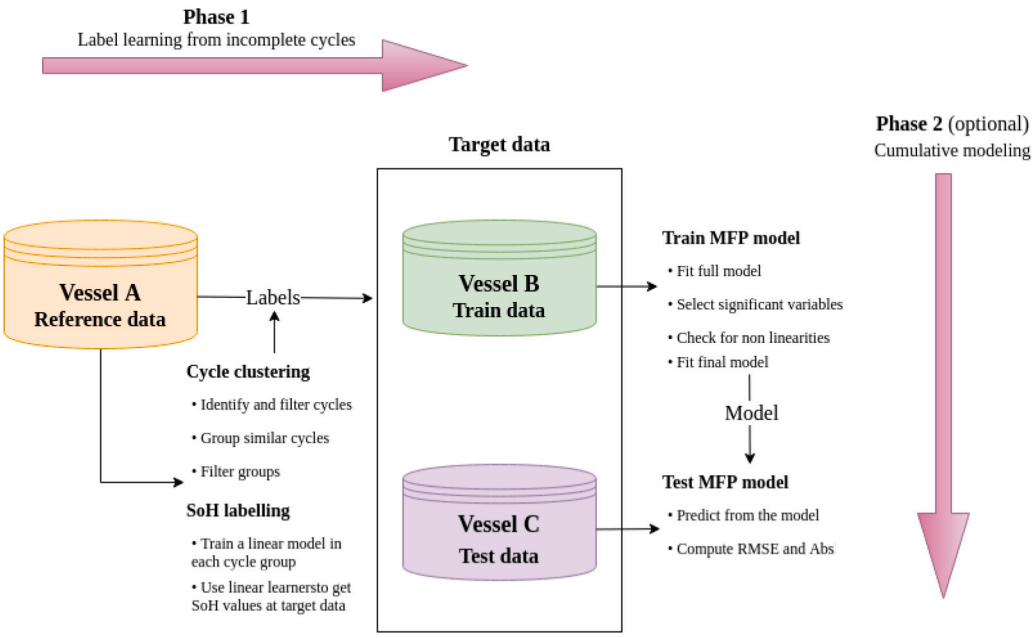

Fig. 3. Visual representation of the data and the various phases of our methodology: reference data from vessel A constitute the references we build the analysis on. Vessels B and C are target data, where we want to obtain SoH estimates. This is done in the first step of the procedure, *label learning from incomplete cycles*, which comprises *cycle clustering* and *SoH labelling*. Once this is achieved, the SoH estimates can be considered as labels for *cumulative modelling*: vessel B becomes a train set and vessel C a test set for a MFP regression model.

desirable to have a weekly or monthly SoH monitoring, it might be convenient to aggregate the estimated SoH accordingly: to this end, a weighted average of the estimated SoH values where the weights are the reciprocal of the uncertainties estimated by the models, as from Eq. (12), is a suitable way to ensure that highly uncertain estimates have little impact to the final SoH labelling.

3.2. Cumulative modelling

The semi-supervised learning procedure we present in this paper enables further supervised data-driven analysis: the newly obtained SoH estimates are used as labels and convert previously unlabelled data into training and test data for constructing and validating the learner.

Among the variety of available data-driven methods (see e.g. [3, 19]), cumulative damages models having the battery capacity degradation as response seem particularly appealing, as they establish a relationship between the factors that accelerate the battery ageing and allow to quantify their effect. Further, they are meaningful for battery systems suppliers when it comes to sizing new products, since the battery size determines the battery capacity, DoD and C-rate which are among the factors that affect the desired lifetime. Encouraged by good results achieved by Multivariable Fractional Polynomials (MFP) regression on data from accelerated tests in a previous work [28], to which we refer for details about the algorithm itself and the main stress factors that can be accounted for by using sensor data, we have here adopted MFP to train a regression model on the data from vessel B, and used vessel C as a test set. In short, MFP is a systematic routine to find the most suitable polynomial by trying different transformations of each covariate from a set of possible choices, with the option of performing variable selection too: we start with a set of candidate covariates and the algorithm selects the best transformation and scaling for those variables that are found to be statistically relevant to predict the response.

The response of our model is the monthly change in the battery SoH with respect to the initial value $\mathrm{SoH}(t_0)$,

$$y = \Delta\mathrm{SoH}(t) = \mathrm{SoH}(t_0) - \mathrm{SoH}(t), \tag{13}$$

where $\mathrm{SoH}(t)$ are the monthly-averaged SoH estimates presented in Section 4.

The candidate covariates we consider to model the degradation are the following:

- An equivalent full cycles measure,
$$efc = \frac{\int_{t_{\mathrm{start}}}^{t_{\mathrm{end}}} |I|\,dt}{C_{\mathrm{nominal}}}, \tag{14}$$
where t_{start} and t_{end} are the initial and final timestamp of the whole operational history, and C_{nominal} is the nominal capacity of the battery;
- A monthly equivalent full cycles measure,
$$efc_{\mathrm{month}} = \frac{\int_{t_1}^{t_2} |I|\,dt}{C_{\mathrm{nominal}}}, \tag{15}$$
where t_1 and t_2 are now the initial and final timestamp of the considered month;
- The monthly average discharge C-rate (absolute value), $\text{C-rate}_{\mathrm{disch.}}$;
- The monthly average charge C-rate (absolute value), $\text{C-rate}_{\mathrm{ch.}}$;
- The monthly average initial voltage of the discharging phases, normalised to the number of modules, $V_{\mathrm{in,\ disch.}}$;
- The monthly average initial voltage of the charging phases, normalised to the number of modules, $V_{\mathrm{in,\ ch.}}$;
- The monthly average voltage difference of the discharging phases, normalised to the number of modules, $\Delta V_{\mathrm{disch.}}$;
- The monthly average voltage difference of the charging phases, normalised to the number of modules $\Delta V_{\mathrm{ch.}}$;
- The monthly averages of the minima and maxima temperature values of each charge and discharge cycles, for every temperature sensor (it is typical to have several temperature sensors in each battery module) $T_{\min,k}$ and $T_{\max,k}$, for $k = 1, \dots, 4$;
- The total duration of the discharging phase during the month, $\Delta t_{\mathrm{disch.}}$;
- The total duration of the charging phase during the month, $\Delta t_{\mathrm{ch.}}$;

- The SoH as estimated in the previous month, SoH_{prev};
- The interaction between efc and C-rate$_{\text{disch.}}$;
- The interaction between one of the minimum temperature, $T_{\text{min},3}$, and C-rate$_{\text{disch.}}$;
- The interaction between $V_{\text{in, disch.}}$ and efc.

Note that all features with the exception of the total efc are cumulative over each month, but not over the entire operational history of the battery system. For this reason, in case of missing data for one whole month inside the operational time span of the battery system, the month itself is not considered for prediction, but the total efc is increased by the average value over all previous months. This correction is enough for the purpose of this paper; however, should it be necessary to obtain predictions at regular intervals without skipping the missing data periods, considering more sophisticated procedures would be needed, e.g. the imputation technique described by Razavi-Far et al. [29].

4. Results

Results from each phase of the semi-supervised learning procedure are presented in this section for one pack of each vessel. Results for other packs of the battery systems are shown in Appendix A.

4.1. Label learning from incomplete cycles

The assumption of constant SoH for N days before and after the independent tests has been adopted with $N = 50$. The choice of N entails a trade-off between accuracy and amount of available reference cycles: in this case, the decision aims at maximising the number of reference cycles, and it is reasonably based on the consideration that the degradation in the first years of vessel operations is still in its linear phase, i.e. it is gentle and slow.

The cycle classification phase provided twelve groups of cycles with similar characteristics for vessel B (however, due to few matches between reference and target cycles, only ten groups were effectively used for the analysis), and seven groups for vessel C. Note that the amount of cycles with similar characteristics, and hence the amount of groups after the classification, is highly dependent on how similar/dissimilar the operational profiles of the considered vessels are. In this case, the matching cycles were shallow and mostly in the range $60\% - 80\%$. However, vessels with closer operational profiles could result in higher numbers of deeper matching cycles. To provide a description of the cycle groups obtained from the cycle classification step, each row of Table 2 displays the shared characteristics of one cycle class.

In the second step of the label learning phase, a linear model has been trained on data from each group of cycles. The selected threshold for the adjusted coefficient of determination is $R^2_{\text{adj}} = 0.6$: in fact, a comparison between the results reported in this section and those in Appendix A obtained with other threshold values (0.5, 0.7, and 0.8) shows that values higher than 0.6 would produce too sparse labels, while $R^2_{\text{adj}} = 0.5$ would include inaccurate and unnecessary estimations.

As an example of the obtained models, two of them, corresponding to groups 1 and 2 described in Table 2, are reported in Tables 3 and 4 respectively. Note that the first model has the minimum considered number of input, due to the presence of scarce reference cycles in group 1, while the second has the full set of input.

The State of Health estimates obtained with our procedure are shown in Figs. 4 and 6 for one pack of vessel B, and in Figs. 5 and 6 for one pack of vessel C. Note that not all the ten groups of cycles (Table 2) were relevant for each of these packs. Combining the contributions of each group, which are shown both separately and altogether in Figs. 4 (vessel B) and 5 (vessel C), the whole (or almost) time span provided with data is covered: the holes in the distributions, in fact, are due to periods of missing data.

The lack of frequent SoH measurements in similar conditions poses a challenge for accuracy assessment. However, the results we achieved are reasonable and entirely in line with the typical degradation behaviour of Li-ion batteries described by Edge et al. (2021, Fig. 17) [23] and Lin et al. (2013, Fig. 2) [30]. The authors describe the battery degradation as constituted by three stages: acceleration, stabilisation (linear ageing) and saturation (nonlinear ageing).

In the results of vessel B it is possible to identify the typical exponential degradation characterising the initial acceleration phase, and it is clear that after the first few months of operations the battery system enters the stabilisation stage, where the degradation is gentle and linear. Recognising the acceleration phase in the results of vessel C is not as easy, due to sparser available data, though some sign of acceleration can be detected in Fig. 6 (right panel), and the linear ageing of the battery system emerges distinctly from the plots. The results are consistent with the batteries having been under operation for less than six years (vessel B) and less than five years (vessel C): in both cases, the saturation stage (third phase, nonlinear ageing) has not been reached yet.

4.2. Cumulative modelling

The MFP models trained on the data from vessel B are reported in Tables 5 and 6: the features of the reduced model (which underwent variable selection) and of the full model, respectively, can be read together with their estimated coefficients, standard errors and corresponding p-values. At a significance level $\alpha = 0.05$, the only inputs that resulted significant are: the total efc, the interaction between the average discharge initial voltage $V_{\text{in, disch.}}$ and the efc itself, and the average minimum temperatures from two sensors, $T_{\text{min},1}$ and $T_{\text{min},3}$. The full model obviously includes all the features presented in Section 3.2, but the vast majority is non-significant. This emerges clearly from Fig. 7: here, the predictions for vessel C obtained from the reduced model (top row) and the full model (bottom row) are compared to the observed values (as estimated from the semi-supervised approach). To evaluate prediction accuracy we provide the normalised Root Mean Squared Error (RMSE),

$$\text{RMSE}_{\text{norm}}(\widehat{\text{SoH}}, \text{SoH}) = \sqrt{\frac{1}{n}\sum_{i=1}^{n}\left(\frac{\text{SoH}_i - \widehat{\text{SoH}}_i}{\text{SoH}_i}\right)^2}, \tag{16}$$

as well as a histogram of the normalised absolute errors,

$$\text{AbsE}_{\text{norm}}(\widehat{\text{SoH}}, \text{SoH})_i = |\text{SoH}_i - \widehat{\text{SoH}}_i|. \tag{17}$$

From Fig. 7 it is clear that, while both models are effective in predicting the SoH degradation, the reduced model is more accurate as the RMSE improves by 1% and all absolute errors are below 2%, while they are mostly between 2%–3% for the full model. Both models, in principle, would be sufficient based on the maritime regulations which usually require errors within 5%. However, it is important to note that the SoH trend estimated by the full model is wrong, since the SoH seems to have an increasing trend over time. The reduced model is therefore a better model, confirming the effectiveness of variable selection.

It is interesting to note that the MFP algorithm has not suggested polynomial transformations for any of the considered input: thus, a linear model would have been equivalent in this case. However, having ensured that there are not significant non-linearities is an important point which would not have been guaranteed by an ordinary linear regression.

5. Discussion and conclusions

This paper presented our novel semi-supervised learning approach to estimate the State of Health of lithium-ion battery systems based on operational sensor data continuously measured from the batteries and a minimal set of weakly labelled data-points. The article is focused on

Table 2
Classes of cycles obtained from the cycle classification step. For each class (each row) we show the shared characteristics of cycles in that group: starting and ending SoC values, average C-rate, variance in the C-rate, minimum and maximum temperatures at the pack level, average pack temperature, temporal and spatial temperature variance.

Index	SoC_{start}	SoC_{end}	C-rate	$\sigma^2_{C\text{-rate}}$	T^{pack}_{min}	T^{pack}_{max}	$\bar{T}^{pack}$	$\bar{\sigma}^2_t$	$\hat{\sigma}^2_{\bar{\mu}^{pack}_t}$
1	72%	52%	−0.56	0.027	33.5 °C	38 °C	34.9 °C	0.48	1.07
2	76%	56%	−0.58	0.025	33 °C	36 °C	34.1 °C	0.31	1.08
3	77%	58%	−0.46	0.021	28 °C	31 °C	28.9 °C	0.29	0.48
4	85%	67%	−0.47	0.013	31 °C	34 °C	31.5 °C	0.11	0.58
5	83%	65%	−0.545	0.026	32 °C	36 °C	33 °C	0.26	0.64
6	86%	66%	−0.53	0.032	34 °C	38 °C	34.9 °C	0.19	0.39
7	88%	69%	−0.53	0.020	30 °C	34 °C	30.6 °C	0.27	0.73
8	88%	71%	−0.35	0.052	29 °C	33 °C	29.9 °C	0.28	0.70
9	87%	69%	−0.50	0.033	36 °C	41 °C	37.3 °C	0.31	1.32
10	89%	67%	−0.284	0.073	22 °C	25 °C	23.4 °C	0.31	1.29

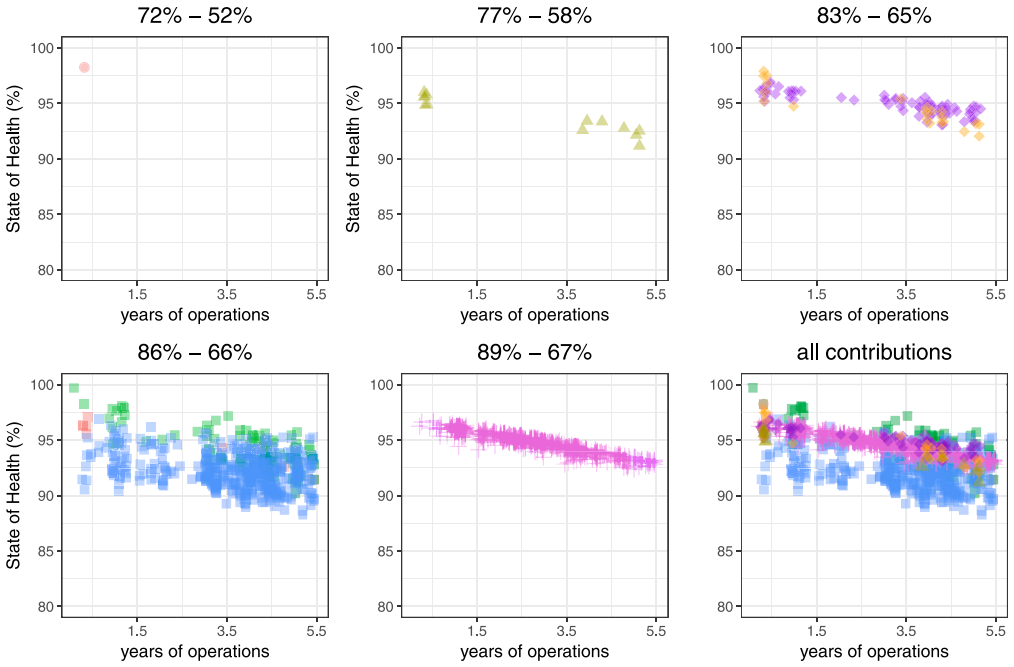

Fig. 4. State of Health estimates for one pack of vessel B. The estimated values are grouped by SoC range (panels 1–5), each colour corresponding to a different group in Table 2. All contributions are plotted together in panel 6. The whole time span provided with data is covered, as holes in the distribution are due to periods of missing data. Larger variance/bias in few groups should be ascribed to poorer models (low R^2_{adj}, see Appendix A) and is reflected in higher uncertainties. Weighted averages (Fig. 6) account for this and therefore constitute a preferable choice. (For interpretation of the references to colour in this figure legend, the reader is referred to the web version of this article.)

Table 3
Linear model trained on reference cycles from group 1. Each feature is reported with the estimated coefficient, standard error and corresponding p-value. The intercept and $C^{(norm)}_{pseudo}$ are normalised to the nominal capacity of the system. The adjusted coefficient of determination is also shown. Note that, in this case, C_{pseudo}, t_{start} and Δt are the only features, since the number of reference cycles in the group was 5 and hence $N < 7$.

	est. coefficient	std. error	p-value
$Intercept^{(norm)}$	1.195	0.19	0.099
$C^{(norm)}_{pseudo}$	−0.004	0.004	0.490
t_{start}	$-2.9 \cdot 10^{-8}$	$1.34 \cdot 10^{-8}$	0.272
Δt	0.02	0.02	0.539
R^2_{adj}		0.78	

Table 4
Linear model trained on reference cycles from group 2. Each feature is reported with the estimated coefficient, standard error and corresponding p-value. The intercept and $C^{(norm)}_{pseudo}$ are normalised to the nominal capacity of the system. The adjusted coefficient of determination is also shown. In this case, the whole set of features is in the model, since there were more than 8 reference cycles (i.e. 12) in the group.

	est. coefficient	std. error	p-value
$Intercept^{(norm)}$	1.07	0.059	$5.6 \cdot 10^{-5}$
$C^{(norm)}_{pseudo}$	0.002	0.002	0.376
t_{start}	$-2.04 \cdot 10^{-8}$	$8.08 \cdot 10^{-9}$	0.065
Δt	$-1.96 \cdot 10^{-3}$	$3.54 \cdot 10^{-3}$	0.607
T^{pack}_{max}	0.52	0.25	0.111
T^{pack}_{min}	−0.36	0.38	0.389
$\bar{\sigma}^2_t$	−1.04	1.85	0.602
σ^2_{C-rate}	−13.6	28.08	0.653
R^2_{adj}		0.67	

battery systems from maritime applications, which are characterised by several differences from batteries in other applications (e.g. electric vehicles or consumer electronics) both in format and operational usage. However, the findings should be reasonably easy to extend to other lithium-ion battery application areas. The results obtained with the semi-supervised learning procedure are in line with the typical degradation patterns of lithium-ion batteries and meet battery experts' expectations. The number and characteristics of similar discharging cycles in each cycle group is highly dependent on how similar the operational profiles of the considered systems are, as well as on the adopted criteria for cycle filtering and clustering. The level at which the analysis is conducted (single cell, module, pack) also has an impact on the predictions. The pack level seemed the most suitable for the data used in this analysis, but depending on the resolution of the data

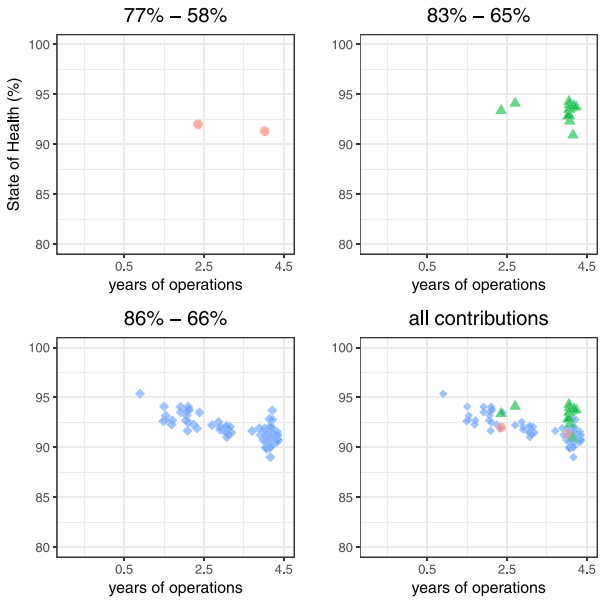

Fig. 5. State of Health estimates for one pack of vessel C. The estimated values are grouped by SoC range (panels 1–3), each colour corresponding to a different group in Table 2. All contributions are plotted together in panel 4. The whole time span provided with data is covered, as holes in the distribution are due to periods of missing data. (For interpretation of the references to colour in this figure legend, the reader is referred to the web version of this article.)

Table 5
Linear model trained on data from vessel B with variable selection. Inputs are derived from the operational sensor data of the battery system; the labels are the monthly averaged SoH estimates obtained with the semi-supervised procedure presented in this paper. The features entering the model are reported together with their estimated coefficients, standard errors and corresponding p-values.

	est. coefficient	std. error	p-value
Intercept	−6.395	1.62	0.0002
efc	0.0008	0.00021	0.0002
$V_{\text{in,disch.}}$: efc	−0.00016	0.00004	0.0005
$T_{\text{min,3}}$	−2.62	0.825	0.0025
$T_{\text{min,1}}$	3.01	0.89	0.0014

Table 6
Linear model trained on data from vessel B without variable selection. Inputs are derived from the operational sensor data of the battery system; the labels are the monthly averaged SoH estimates obtained with the semi-supervised procedure presented in this paper. All features are reported together with their estimated coefficients, standard errors and corresponding p-values.

	est. coefficient	std. error	p-value
Intercept	−67.24	45.37	0.1472
efc	0.016	0.006	0.0137
$V_{\text{in,disch.}}$: efc	−0.003	0.001	0.0156
$T_{\text{min,3}}$	−60	28.19	0.0790
$T_{\text{min,1}}$	43.67	24.32	0.0812
$T_{\text{max,1}}$	−41.03	24.73	0.1059
$T_{\text{max,3}}$	43.59	28.54	0.1356
$\Delta V_{\text{ch.}}$	−0.087	0.07	0.2215
$\Delta t_{\text{ch.}}$	−0.003	0.002	0.2324
SoH_{prev}	0.18	0.15	0.2416
$\Delta t_{\text{disch.}}$	−0.0015	0.0015	0.3288
$V_{\text{in,disch.}}$	2.01	2.44	0.4156
$\Delta V_{\text{disch.}}$	−0.06	0.07	0.4211
efc : $\text{C} - \text{rate}_{\text{disch.}}$	−0.0007	0.0009	0.4519
$T_{\text{min,4}}$	15.77	24.74	0.5278
$T_{\text{max,4}}$	−15.36	24.57	0.5358
$T_{\text{max,2}}$	12.06	23.61	0.6127
$V_{\text{in,ch.}}$	−1.12	2.42	0.6457
$T_{\text{min,2}}$	−7.23	22.9	0.7540
$\text{C} - \text{rate}_{\text{disch.}}$	7.45	29.6	0.8027
$\text{efc}_{\text{month}}$	0.0007	0.003	0.8407
$\text{C} - \text{rate}_{\text{ch.}}$	0.7	4.44	0.8758
$T_{\text{min,2}}$: $\text{C} - \text{rate}_{\text{disch.}}$	−0.05	1.06	0.9642

at cell or module level, other choices could, in general, be possible and preferable. Another aspect which is crucial for the procedure success is the availability and reliability of the State of Charge estimates. In the present case, accurate and frequent State of Charge measurements were provided by the data supplier company and we could build our analysis on such data just as if they were sensor data; however, generally speaking the correct estimation of the State of Charge is a demanding task and it might have some uncertainties. The strength of our method resides in the capability of assessing the State of Health of one or more battery systems on the basis of a very few State of Health observations for a similar system, profitably extracting information from large amounts of unlabelled data. A main asset of the procedure is also having being designed on data gathered from real operation, as opposed to the many SoH algorithms in the literature that are designed and tested on lab data only. As a matter of fact, it would be possible for our method to be trained on lab data and then applied on operational data, provided that the same kind of battery is tested in the laboratory and operated in real world: this could have been considered e.g. for lack of "real reference" data (in our case, if we had not have a vessel with three SoH test available). However, when possible, we would advice to consider operational data both as reference and target, since the method is fully data-driven and a fundamental point in statistics and data science is that training and test data should come from the same distribution. Finally, our method is characterised by a high versatility. In fact, the first part of the method, label learning from incomplete cycles, can be used *per se*, to obtain State of Health estimates both in an online or offline setup. Additionally, it can be exploited for transforming unlabelled data into training/test data for supervised learning, e.g. anomaly detection or cumulative degradation modelling. As an example, in the second phase we have applied the Multivariable Fractional Polynomial algorithm to model the monthly variation in the battery SoH compared to the initial SoH of the battery. The achieved results are encouraging, as the normalised Root Mean Squared Error is less than 1% and almost all the normalised absolute errors are below 1.5% for the reduced model. The missing data issue, which is the typical obstacle for cumulative damage models which are based on the whole operational history of the battery system, was overcome by increasing the equivalent full cycle measure in the months with no data at all, by the average value of the previous months; more sophisticated procedures would be needed in order to obtain predictions at regular intervals, without skipping periods of missing data.

An interesting development for future works is certainly to try and perfect the method on datasets with longer operational time spans, that is, reflecting a more advanced battery degradation. At the same time, adapting the procedure to lithium-ion batteries from other areas than the maritime field would be attractive and valuable.

CRediT authorship contribution statement

Clara Bertinelli Salucci: Conceptualization, Methodology, Software, Validation, Formal analysis, Writing – original draft, Writing – review & editing, Visualization. **Azzeddine Bakdi:** Conceptualization, Methodology, Validation, Writing – review & editing, Visualization, Supervision. **Ingrid Kristine Glad:** Conceptualization, Methodology, Validation, Writing – review & editing, Visualization, Supervision, Project administration, Funding acquisition. **Erik Vanem:** Conceptualization, Methodology, Validation, Writing – review & editing, Visualization, Supervision. **Riccardo De Bin:** Conceptualization, Methodology, Validation, Writing – review & editing, Visualization, Supervision, Project administration.

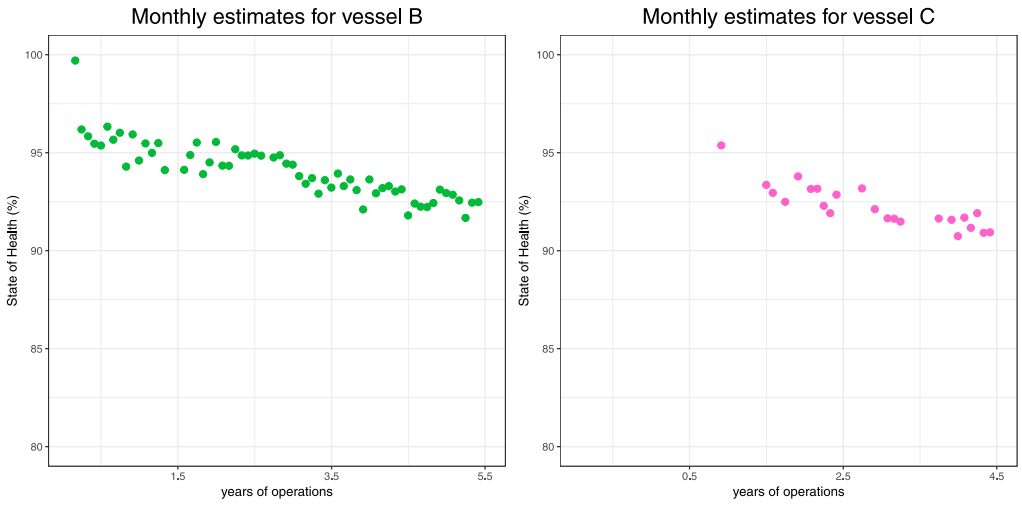

Fig. 6. Left: Monthly weighted averages of the estimates for vessel B shown in Fig. 4. Right: Monthly weighted averages of the estimates for vessel C shown in Fig. 5. In both cases, the weights are the reciprocal of the uncertainties estimated by the models, to ensure that highly uncertain estimates have little impact to the final estimate.

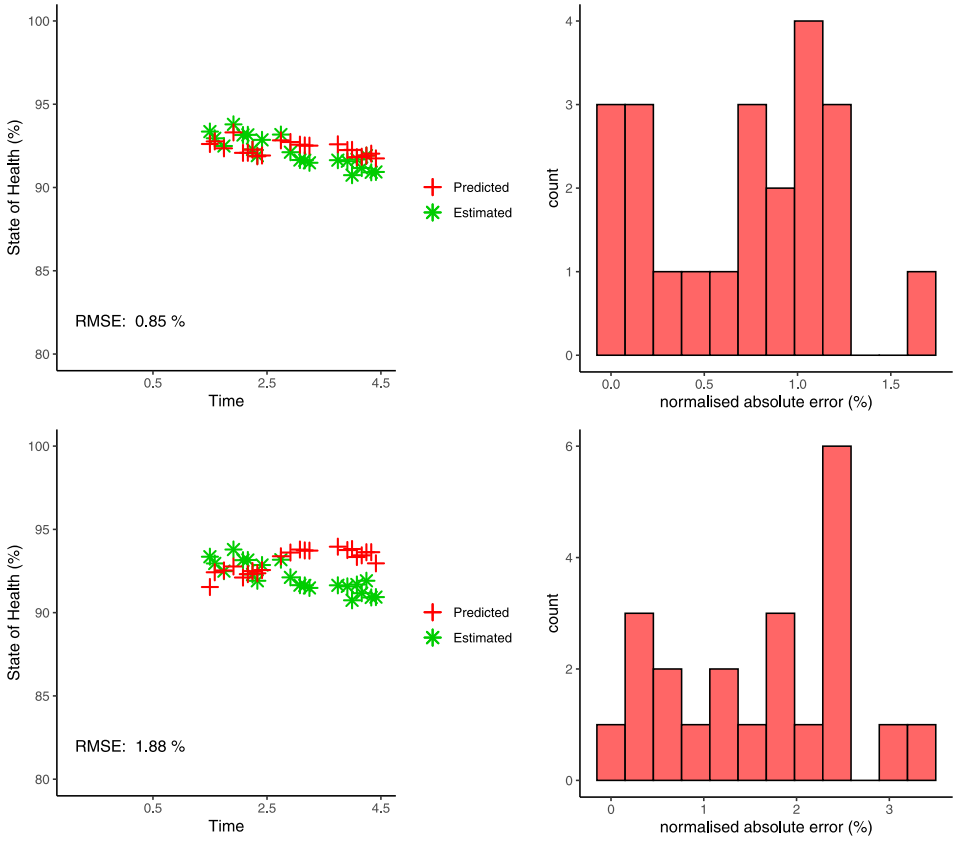

Fig. 7. Left plots: State of Health degradation results for vessel C using the MFP regression model trained on data from vessel B, with variable selection (top) or without (bottom). Right plots: histogram of the normalised absolute error obtained with the reduced model (top) and with the full model (bottom).

Declaration of competing interest

The authors declare that they have no known competing financial interests or personal relationships that could have appeared to influence the work reported in this paper.

Data availability

The data that has been used is confidential.

Acknowledgements

This research is funded by the Norwegian Research Council research-based innovation center BigInsight, project no 237718.

We thank Lars Ole Valøen, Kandepu Rambabu and Chi Tsang (Corvus Energy) for having provided data and support for this project, Øystein Åsheim Alnes (DNV) for his expertise and insight that helped improving the research, and Terje Kvernes (UiO) for the great IT support.

Appendix A. Supplementary data

Supplementary material related to this article can be found online at https://doi.org/10.1016/j.jpowsour.2022.232429.

References

[1] Aviation and shipping — impacts on Europe's environment, 2017, https://www.eea.europa.eu/publications/term-report-2017.
[2] C. Sbarufatti, M. Corbetta, M. Giglio, F. Cadini, Adaptive prognosis of lithium-ion batteries based on the combination of particle filters and radial basis function neural networks, J. Power Sources 344 (2017) 128–140.
[3] E. Vanem, C. Bertinelli Salucci, A. Bakdi, A. Øystein Åsheim, Data-driven state of health modelling—A review of state of the art and reflections on applications for maritime battery systems, J. Energy Storage 43 (2021) 103158.
[4] A. Basia, Z. Simeu-Abazi, E. Gascard, P. Zwolinski, Review on state of health estimation methodologies for lithium-ion batteries in the context of circular economy, CIRP J. Manuf. Sci. Technol. 32 (2021) 517–528.
[5] L. Yao, S. Xu, A. Tang, F. Zhou, J. Hou, Y. Xiao, Z. Fu, A review of lithium-ion battery state of health estimation and prediction methods, World Electr. Veh. J. 12 (3) (2021).
[6] H. Tian, P. Qin, K. Li, Z. Zhao, A review of the state of health for lithium-ion batteries: Research status and suggestions, J. Clean. Prod. 261 (2020) 120813.
[7] A. Barré, B. Deguilhem, S. Grolleau, M. Gérard, F. Suard, D. Riu, A review on lithium-ion battery ageing mechanisms and estimations for automotive applications, J. Power Sources 241 (2013) 680–689.
[8] M.U. Cuma, T. Koroglu, A comprehensive review on estimation strategies used in hybrid and battery electric vehicles, Renew. Sustain. Energy Rev. 42 (2015) 517–531.
[9] A. Farmann, W. Waag, A. Marongiu, D.U. Sauer, Critical review of on-board capacity estimation techniques for lithium-ion batteries in electric and hybrid electric vehicles, J. Power Sources 281 (2015) 114–130.
[10] M. Berecibar, I. Gandiaga, I. Villarreal, N. Omar, J. Van Mierlo, P. Van den Bossche, Critical review of state of health estimation methods of Li-ion batteries for real applications, Renew. Sustain. Energy Rev. 56 (2016) 572–587.
[11] Y. Li, K. Liu, A.M. Foley, A. Zülke, M. Berecibar, E. Nanini-Maury, J. Van Mierlo, H.E. Hoster, Data-driven health estimation and lifetime prediction of lithium-ion batteries: A review, Renew. Sustain. Energy Rev. 113 (2019) 109254.
[12] R. Xiong, J. Tian, W. Shen, J. Lu, F. Sun, Semi-supervised estimation of capacity degradation for lithium ion batteries with electrochemical impedance spectroscopy, J. Energy Chem. (2022).
[13] Y. Che, D.-I. Stroe, X. Hu, R. Teodorescu, Semi-supervised self-learning-based lifetime prediction for batteries, IEEE Trans. Ind. Inform. (2022) 1–10.
[14] Y. Li, H. Sheng, Y. Cheng, D.-I. Stroe, R. Teodorescu, State-of-health estimation of lithium-ion batteries based on semi-supervised transfer component analysis, Appl. Energy 277 (2020) 115504.
[15] Z. Deng, X. Lin, J. Cai, X. Hu, Battery health estimation with degradation pattern recognition and transfer learning, J. Power Sources 525 (2022) 231027.
[16] Y. Li, K. Li, X. Liu, Y. Wang, L. Zhang, Lithium-ion battery capacity estimation - A pruned convolutional neural network approach assisted with transfer learning, Appl. Energy 285 (2021) 116410.
[17] J. Yu, J. Yang, Y. Wu, D. Tang, J. Dai, Online state-of-health prediction of lithium-ion batteries with limited labeled data, Int. J. Energy Res. 44 (14) (2020) 11345–11360.
[18] Y. Wu, W. Li, Online capacity estimation for lithium-ion batteries based on semi-supervised convolutional neural network, World Electr. Veh. J. 12 (4) (2021).
[19] W. Diao, I.H. Naqvi, M. Pecht, Early detection of anomalous degradation behavior in lithium-ion batteries, J. Energy Storage 32 (2020) 101710.
[20] P. Weicker, A Systems Approach to Lithium-Ion Battery Management, Artech House, 2013.
[21] DNV GL handbook for maritime and offshore battery systems, 2016, Report No.: 2016-1056, Revision: V1.0, Document No.: 15DJV2L-2. https://sustainableworldports.org/wp-content/uploads/DNV-GL_2016-Handbook-maritime-offshore-battery-systems-report.pdf.
[22] M. Dubarry, C. Pastor-Fernández, G. Baure, T.F. Yu, W.D. Widanage, J. Marco, Battery energy storage system modeling: Investigation of intrinsic cell-to-cell variations, J. Energy Storage 23 (2019) 19–28.
[23] J.S. Edge, S. O'Kane, R. Prosser, N.D. Kirkaldy, A.N. Patel, A. Hales, A. Ghosh, W. Ai, J. Chen, J. Yang, S. Li, M.-C. Pang, L. Bravo Diaz, A. Tomaszewska, M.W. Marzook, K.N. Radhakrishnan, H. Wang, Y. Patel, B. Wu, G.J. Offer, Lithium ion battery degradation: what you need to know, Phys. Chem. Chem. Phys. 23 (2021) 8200–8221.
[24] S. Zhang, X. Guo, X. Dou, X. Zhang, A rapid online calculation method for state of health of lithium-ion battery based on coulomb counting method and differential voltage analysis, J. Power Sources 479 (2020) 228740.
[25] H.J. Kim, K.H. Kwak, Absolute capacity estimation method with temperature effect for a small lithium-polymer battery, J. Korea Inst. Mil. Sci. Technol. 19 (2016) 26–34.
[26] A. Azzalini, B. Scarpa, Data Analysis and Data Mining: An Introduction, Oxford University Press, 2012, pp. 15–38.
[27] A.K. Srivastava, V.K. Srivastava, A. Ullah, The coefficient of determination and its adjusted version in linear regression models, Econometric Rev. 14 (2) (1995) 229–240.
[28] C. Bertinelli Salucci, A. Bakdi, I.K. Glad, E. Vanem, R. De Bin, Multivariable fractional polynomials for lithium-ion batteries degradation models under dynamic conditions, J. Energy Storage 52 (2022) 104903.
[29] R. Razavi-Far, S. Chakrabarti, M. Saif, E. Zio, An integrated imputation-prediction scheme for prognostics of battery data with missing observations, Expert Syst. Appl. 115 (2019) 709–723.
[30] X. Lin, J. Park, L. Liu, Y. Lee, A. Sastry, W. Lu, A comprehensive capacity fade model and analysis for li-ion batteries, J. Electrochem. Soc. 160 (2013) A1701–A1710.